POLITECNICO DI TORINO
Repository ISTITUZIONALE

Approximation of anisotropic multilayered plates through RMVT and MITC elements.

Original
Approximation of anisotropic multilayered plates through RMVT and MITC elements / Chinosi, C., DELLA CROCE, L., Cinefra, M., Carrera, E.. - In: COMPOSITE STRUCTURES. - ISSN 0263-8223. - 158:(2016), pp. 252-261. [10.1016/j.compstruct.2016.09.032]

Availability:
This version is available at: 11583/2650614 since: 2016-09-26T14:28:19Z

Publisher:
Elsevier

Published
DOI:10.1016/j.compstruct.2016.09.032

Terms of use:

This article is made available under terms and conditions as specified in the corresponding bibliographic description in the repository

Publisher copyright

(Article begins on next page)

15 October 2026

Approximation of anisotropic multilayered plates through RMVT and MITC elements

Claudia Chinosi[a], Lucia Della Croce[b], Maria Cinefra[c,*], Erasmo Carrera[c]

[a] *Department of Sciences and Technological Innovation, Università del Piemonte Orientale, Alessandria, Italy*
[b] *Department of Mathematics, Università di Pavia, Pavia, Italy*
[c] *Aerospace Engineering Department, Politecnico di Torino, Torino, Italy*

Abstract

This paper presents a mixed two dimensional model for the analysis of mechanical response in anisotropic multilayered plates, with particular attention to the behavior along the thickness of the plate. It is well known that the study of anisotropic material structures requires to take into account cross-elasticity effects that make the solution converge very slowly. The finite element method showed successful performances to approximate the solutions of these structures. In this regard, two variational formulations are available to calculate the stiffness matrix, the Principle of Virtual Displacement (PVD) and the Reissner Mixed Variational Theorem (RMVT). Here, a strategy similar to MITC (Mixed Interpolated of Tensorial Components) approach, in the RMVT formulation, is adopted to formulate advanced locking-free finite elements. Then, assuming the transverse stresses as independent variables, the continuity at the interfaces between layers is easily imposed. The displacement field is defined according to the Reissner-Mindlin theory and the shear stresses are assumed parabolic along the thickness by means of RMVT. The normal strain ϵ_{zz} and the normal stress σ_{zz} are discarded. The shear stresses σ_{xz} and σ_{yz} are interpolated in each element according to the MITC. By comparing the results with benchmark solutions from literature, it is shown that the element exhibits both properties of convergence and robustness and provides very accurate results in terms of transverse shear stresses of the anisotropic multilayered plate.

Key words: Anisotropic plates, Finite Elements, Mixed Interpolation of Tensorial Components, Reissner Mixed Variational Theorem;

1. Introduction

With the development of high performance fiber reinforced composite materials for structural applications has come an increased interest in solutions to anisotropic plate problems. A large number of solutions exist for bending, buckling, and free vibration of specially orthotropic rectangular plates in which the principal elastic axes are parallel to the sides of the plate. Many of these solutions are summarized in References [1]-[3],

In most structural applications, however, fiber reinforced composites are constructed of unidirectional plies in which the fiber axis is oriented at an angle θ to the x axis as illustrated in Figure 1. For such a composite symmetrically laminated about the mid-plane, the bending response is governed by the flexural equation of a homogeneous anisotropic plate [4, 5], including the cross-elasticity bending stiffness terms D_{16} and D_{26}. Moreover, a number of complicating effects arise in the analysis of multilayered composite structures due to the intrinsic discontinuity of the mechanical properties at each layer–interface to which high shear and normal transverse deformability is associated. An accurate description of the stress and strain fields of these structures requires theories that are able to satisfy the so–called Interlaminar Continuity (IC) conditions for the transverse stresses (see Whitney [6], and Pagano [7], as examples).

Transverse anisotropy of multilayered structures make it difficult to find closed form solutions and the use of approximated solutions is necessary. It can therefore be concluded that the use of both refined two–dimensional theories and computational methods become mandatory to solve practical problems related to multilayered anisotropic structures. Among the several available computational methods, the Finite Element Method (FEM) has played and continues to play a significant role. In this work, the Reissner's Variational Mixed Theorem (RMVT) is used to derive plate finite elements. As a main property, RMVT permits one to assume two independent fields for diplacement and transverse stress variables. The resulting advanced finite elements therefore describe *a priori* interlaminar continuous transverse stress fields.

For a complete and rigorous understanding of the foundations of RMVT, reference can be made to the articles by

*Corresponding author.
Email addresses: maria.cinefra@polito.it (Erasmo Carrera)

Professor Reissner [8]-[10] and the review article by Carrera [11]. The first application of RMVT to modeling of multilayered flat structures was performed by Murakami [12],[13]. He introduced a first order displacement field in his papers, in conjunction with an independent parabolic transverse stress LW field in each layer (transverse normal stress and strain were discarded). An extension to a higher order displacement field was proposed by Toledano and Murakami in [14]. While in [15], they extended the RMVT to a layer-wise description of both displacement and transverse stress fields. These papers [12]-[15] should be considered as the fundamental works in the applications of RMVT as a tool to model multilayered structures. Further discussions on RMVT were provided by Soldatos [16]. A generalization, proposing a systematic use of RMVT as a tool to furnish a class of two dimensional theories for multilayered plate analysis, was presented by Carrera [17]-[19]. The order of displacement fields in the layer was taken as a free parameter of the theories. Applications of what is reported in [17],[18] have been given in several other papers [20]-[27], in which closed-form solution are considered. Layer-wise mixed analyses were performed in [28] for the static case. As a fundamental result, the numerical analysis demonstrated that RMVT furnishes a quasi three-dimensional a priori description of transverse stresses, including transverse normal components. Sandwich plates were also considered in [21]. Recently, Messina [29] has compared RMVT results to PVD (Principle of Virtual Displacements) ones. Transverse normal stresses were, however, discarded in this work. In [30]-[32], Carrera and Demasi developed multilayered plate elements based on RMVT, that were able to give a quasi–three-dimensional description of stress/strain fields. But in these works, they still employ the selective reduced integration [33] to overcome the shear locking phenomenon.

Recently, authors adopted the Mixed Interpolation of Tensorial Components (MITC) to contrast the locking. According to this technique, the strain components are not directly computed from the displacements but they are interpolated within each element using a specific interpolation strategy for each component. For more details about MITC, the readers can refer to the works [34]-[38]. In [39], the authors formulated plate/shell elements based on displacement formulation that showed good properties of convergence thanks to the use of the MITC. Then in [40], they adopted the same strategy of the MITC to interpolate the transverse stresses that are modelled a-priori by the RMVT. In this way, they demonstrated that IC conditions are satisfied and the shear locking is contrasted at the same time, by means of the RMVT. The plate elements proposed in [40] have nine nodes. The displacement field is defined according to the Reissner-Mindlin theory and the shear stresses are assumed parabolic along the thickness by means of RMVT. The normal strain ϵ_{zz} and the normal stress σ_{zz} are discarded. The shear stresses σ_{xz} and σ_{yz} are interpolated in each element according to the MITC.

This paper presents the extension of the plate elements in [40], formulated for the analysis of isotropic multilayered structures, to the analysis of anisotropic multilayered plates. It is here demonstrated that these elements not only satisfy IC conditions but they also take into account the cross-elasticity effects of anisotropic materials providing good results in terms of transverse shear stresses. Plate finite elements based on Reissner-Mindlin assumptions and displacement formulation are considered for comparison purposes. Comparisons with 3D solutions are also provided. Future companion works will be devoted to the higher order RMVT models and the analysis of anisotropic multilayered shell structures.

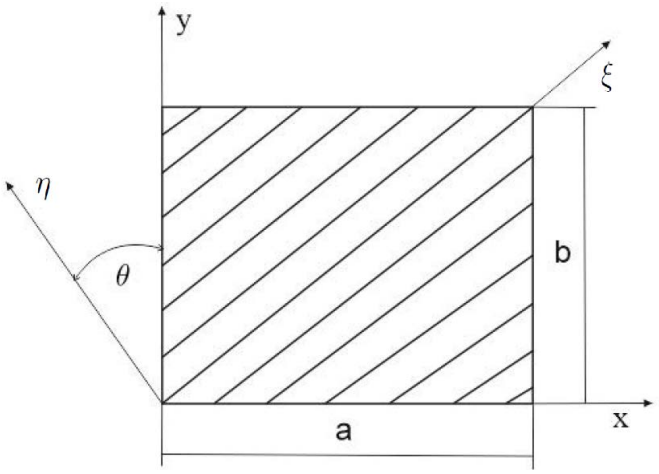

Figure 1: Unidirectional ply.

2. Anisotropic multilayered materials

The *constitutive* equations describing the relations between the stress tensor $\tilde{\sigma} = \sigma_{ij},\ i,j = 1,\dots 3$ and the strain tensor $\tilde{\varepsilon} = \varepsilon_{ij},\ i,j = 1,\dots 3$ for linear elastic materials are given by the generalized Hooke's law:

$$\sigma_{ij} = \tilde{C}_{ijhk}\varepsilon_{hk},\ i,j,h,k = 1,...3, \tag{1}$$

where $\tilde{C}_{ijhk}$ is the fourth-order elasticity tensor of material constants. Referring to the reference system (ξ,η,ζ) of the material, we introduce the stress vector:

$$\hat{\boldsymbol{\sigma}} = [\sigma_{\xi\xi}\ \sigma_{\eta\eta}\ \sigma_{\xi\eta}\ \sigma_{\xi\zeta}\ \sigma_{\eta\zeta}\ \sigma_{\zeta\zeta}]^T$$

and analogously the strain vector:

$$\hat{\boldsymbol{\epsilon}} = [\epsilon_{\xi\xi}\ \epsilon_{\eta\eta}\ \epsilon_{\xi\eta}\ \epsilon_{\xi\zeta}\ \epsilon_{\eta\zeta}\ \epsilon_{\zeta\zeta}]^T,$$

assuming that:

$$\epsilon_{\xi\eta} = \varepsilon_{12} + \varepsilon_{21}, \epsilon_{\xi\zeta} = \varepsilon_{13} + \varepsilon_{31},\ \epsilon_{\eta\zeta} = \varepsilon_{23} + \varepsilon_{32}.$$

For orthotropic materials, the Hooke's law (1) can be written in the matrix form $\hat{\boldsymbol{\sigma}} = \mathrm{C}\hat{\boldsymbol{\epsilon}}$, where the elasticity matrix C is symmetric with 9 independent coefficients:

$$\begin{bmatrix} \sigma_{\xi\xi} \\ \sigma_{\eta\eta} \\ \sigma_{\xi\eta} \\ \sigma_{\xi\zeta} \\ \sigma_{\eta\zeta} \\ \sigma_{\zeta\zeta} \end{bmatrix} = \begin{bmatrix} C_{11} & C_{12} & 0 & 0 & 0 & C_{13} \\ & C_{22} & 0 & 0 & 0 & C_{23} \\ & & C_{66} & 0 & 0 & 0 \\ & & & C_{44} & 0 & 0 \\ & sym & & & C_{55} & 0 \\ & & & & & C_{33} \end{bmatrix} \begin{bmatrix} \epsilon_{\xi\xi} \\ \epsilon_{\eta\eta} \\ \epsilon_{\xi\eta} \\ \epsilon_{\xi\zeta} \\ \epsilon_{\eta\zeta} \\ \epsilon_{\zeta\zeta} \end{bmatrix}, \tag{2}$$

We observe that the indices order in C refers to the classical *Voigt-Kelvin* notation.

In this paper we consider laminated structures made of N_l orthotropic laminae that are supposed to be perfectly bonded together. Let the structure occupies a region $V = \Omega \times (-\frac{t}{2}, \frac{t}{2})$, where Ω is the middle surface and $t > 0$ is the thickness of the plate. We assume Ω as reference surface of the laminated plate. The k-layer is described by the ζ_k, ζ_{k+1} coordinates respect to the reference surface and by the thickness $t_k = \zeta_{k+1} - \zeta_k$ with

$$t = \sum_{k=1}^{N_l} t_k.$$

Multilayered structures are often composed of layers made up with different orientations. Therefore it needs to write the previous relations from the reference system (ξ, η, ζ) into the reference problem system (x, y, z). Assuming that the two systems have the same origin and the ζ and z-axes are coincident, the classical coordinate transformation reads:

$$\begin{bmatrix} \xi \\ \eta \\ \zeta \end{bmatrix} = \begin{bmatrix} \cos\theta & \sin\theta & 0 \\ -\sin\theta & \cos\theta & 0 \\ 0 & 0 & 1 \end{bmatrix} \begin{bmatrix} x \\ y \\ z \end{bmatrix}, \tag{3}$$

where θ is the angle which the ξ-axis forms with the x-axis counterclockwise. Let $\boldsymbol{\sigma}$ and $\boldsymbol{\epsilon}$ be the stress and strain vector in the reference problem system (x, y, z), respectively. For each layer the stress and the strain transformations hold and the constitutive law in the reference problem system reads as:

$$\boldsymbol{\sigma}^{(k)} = \bar{\mathrm{C}}^{(k)} \boldsymbol{\epsilon}^{(k)}. \tag{4}$$

that in explicit form is:

$$\begin{bmatrix} \sigma_{xx} \\ \sigma_{yy} \\ \sigma_{xy} \\ \sigma_{xz} \\ \sigma_{yz} \\ \sigma_{zz} \end{bmatrix} = \begin{bmatrix} \bar{C}_{11} & \bar{C}_{12} & \bar{C}_{16} & 0 & 0 & \bar{C}_{13} \\ & \bar{C}_{22} & \bar{C}_{26} & 0 & 0 & \bar{C}_{23} \\ & & \bar{C}_{66} & 0 & 0 & \bar{C}_{63} \\ & & & \bar{C}_{44} & \bar{C}_{45} & 0 \\ & sym & & & \bar{C}_{55} & 0 \\ & & & & & \bar{C}_{33} \end{bmatrix} \begin{bmatrix} \epsilon_{xx} \\ \epsilon_{yy} \\ \epsilon_{xy} \\ \epsilon_{xz} \\ \epsilon_{yz} \\ \epsilon_{zz} \end{bmatrix}, \tag{5}$$

Note that the coefficients $\bar{C}_{16}$, $\bar{C}_{26}$, $\bar{C}_{36}$ and $\bar{C}_{45}$ appear.

3. RMVT formulation

The analysis of multilayered structures is difficult when compared to one-layered ones. A number of complicating effects arise when their mechanical behavior as well as failure mechanisms have to be correctly understood. This is due to the intrinsic discontinuity of the mechanical properties at each layer–interface to which high shear and normal transverse deformabilty is associated. An accurate description of the stress and strain fields of these structures requires theories that are able to satisfy the so–called Interlaminar Continuity (IC) conditions for the transverse stresses (see Whitney [6], and Pagano [7], as examples). Among these theories, the variational statement RMVT has been usefully employed to modeling of multilayered flat structures (see e.g. [12], [15] and the references therein).

3.1. The one-layered plate

Here we deal with the description of stress and strain fields in the $k-$th lamina of a multilayered plate subjected to static loadings. As a main property, RMVT permits one to assume two independent fields for diplacement and transverse stress variables and thus enables one to describe *a priori* interlaminar continuous transverse stress fields. Following this approach the stress and the strain vectors are written in terms of the in-plane and transverse components (for semplicity we omit the index k) :

$$\hat{\boldsymbol{\sigma}} = [\hat{\boldsymbol{\sigma}}_p \;\; \hat{\boldsymbol{\sigma}}_n], \quad \hat{\boldsymbol{\epsilon}} = [\hat{\boldsymbol{\epsilon}}_p \;\; \hat{\boldsymbol{\epsilon}}_n] \tag{6}$$

Further subscripts H, G and M are introduced. H means that the stresses are computed by Hooke's law, G means that the strains are computed from geometrical relations and M stands for *Model*. Let us suppose that the lamina occupies a region $V_k = \Omega \times (-\frac{t_k}{2}, \frac{t_k}{2})$ and that it is subjected to external layer force $\mathbf{p}$. Thus, in the reference lamina system, the RMVT formulation can be written as follows:

$$\int_{V_k} \left[\delta\hat{\boldsymbol{\epsilon}}_{pG} \hat{\boldsymbol{\sigma}}_{pH} + \delta\hat{\boldsymbol{\epsilon}}_{nG} \hat{\boldsymbol{\sigma}}_{nM} + \delta\hat{\boldsymbol{\sigma}}_{nM} (\hat{\boldsymbol{\epsilon}}_{nG} - \hat{\boldsymbol{\epsilon}}_{nH}) \right] d\xi d\eta d\zeta = \delta L_e \tag{7}$$

where the third term variationally enforces the compatibility condition of the transverse strains $\hat{\boldsymbol{\epsilon}}_{nG} = \hat{\boldsymbol{\epsilon}}_{nH}$ and δL_e is the virtual variation of the work made by $\mathbf{p}$. Now we take into account the Reissner-Mindlin assumption, $\sigma_{\zeta\zeta} = 0$, ([41], [42]) which implies that the transverse stress vector is reduced to a two components vector:

$$\hat{\boldsymbol{\sigma}}_{nM} = [\sigma_{\xi\zeta} \;\; \sigma_{\eta\zeta}] \tag{8}$$

and that the strain component $\epsilon_{\zeta\zeta}$ can be neglected. Thus the constitutive relations (5) are decoupled in the in-plane and out-of-plane components in this way:

$$\begin{bmatrix} \sigma_{\xi\xi} \\ \sigma_{\eta\eta} \\ \sigma_{\xi\eta} \end{bmatrix} = \begin{bmatrix} C_{11} & C_{12} & C_{16} \\ & C_{22} & C_{26} \\ sym & & C_{66} \end{bmatrix} \begin{bmatrix} \epsilon_{\xi\xi} \\ \epsilon_{\eta\eta} \\ \epsilon_{\xi\eta} \end{bmatrix} \tag{9}$$

$$\begin{bmatrix} \sigma_{\xi\zeta} \\ \sigma_{\eta\zeta} \end{bmatrix} = \begin{bmatrix} C_{44} & C_{45} \\ sym & C_{55} \end{bmatrix} \begin{bmatrix} \epsilon_{\xi\zeta} \\ \epsilon_{\eta\zeta} \end{bmatrix}. \tag{10}$$

Let $\mathrm{C_{pp}}$ and $\mathrm{C_{nn}}$ be the elasticity matrices in (9) and (10) respectively, we can write:

$$\hat{\boldsymbol{\sigma}}_{pH} = \mathrm{C_{pp}}\hat{\boldsymbol{\epsilon}}_{pG}, \quad \hat{\boldsymbol{\sigma}}_{nM} = \mathrm{C_{nn}}\hat{\boldsymbol{\epsilon}}_{nH} \tag{11}$$

and expressing $\hat{\boldsymbol{\epsilon}}_{nH}$ in terms of the independent variable $\hat{\boldsymbol{\sigma}}_{nM}$ we have:

$$\hat{\boldsymbol{\epsilon}}_{nH} = (\mathrm{C_{nn}})^{-1}\hat{\boldsymbol{\sigma}}_{nM}. \tag{12}$$

Upon substitution of the first of (11) and of (12) into (7) we obtain the variational formulation in RMVT framework:

$$\begin{aligned} \int_{V_k} \big[& \delta\hat{\boldsymbol{\epsilon}}_{pG}\,\mathrm{C_{pp}}\,\hat{\boldsymbol{\epsilon}}_{pG} + \delta\hat{\boldsymbol{\epsilon}}_{nG}\hat{\boldsymbol{\sigma}}_{nM} + \\ & \delta\hat{\boldsymbol{\sigma}}_{nM}\left(\hat{\boldsymbol{\epsilon}}_{nG} - (\mathrm{C_{nn}})^{-1}\hat{\boldsymbol{\sigma}}_{nM}\right)\big]\, d\xi d\eta d\zeta = \delta L_e \end{aligned} \tag{13}$$

In the case that the $k-$th lamina is orthotropic The elastic coefficients of the matrices $\mathrm{C_{pp}}$ and $\mathrm{C_{nn}}$ are experimentally determined in terms of engineering constants such as the Young modulus E, the transverse elasticity modulus G and the Poisson's ratio ν. They are:

$$\mathrm{C_{pp}} = \begin{bmatrix} \dfrac{E_1}{1-\nu_{12}\nu_{21}} & \dfrac{E_2\nu_{12}}{1-\nu_{12}\nu_{21}} & 0 \\ & \dfrac{E_2}{1-\nu_{12}\nu_{21}} & 0 \\ sym & & G_{12} \end{bmatrix}, \tag{14}$$

$$\mathrm{C_{nn}} = \begin{bmatrix} G_{13} & 0 \\ 0 & G_{23} \end{bmatrix}. \tag{15}$$

where $E_1,\ E_2,\ \nu_{12},\ \nu_{21}$ are the Young modulus and the Poisson's ratio, respectively, in the $\xi,\ \eta$ directions of the lamina system and are linked to each other by: $\nu_{21}/E_2 = \nu_{12}/E_1$. $G_{13},\ G_{23},\ G_{12}$ are the transverse elasticity modulus in the planes $(\xi\ \zeta),\ (\eta\ \zeta),\ (\xi\ \eta)$ respectively.

3.2. The anisotropic multilayered plate

The splitting of the Hooke's law (11) in the in-plane and out-of-plane components leads to write the relation (4) for the k-th lamina in the following form:

$$\boldsymbol{\sigma}^{(k)}_{pH} = \bar{\mathrm{C}}^{(k)}_{\mathrm{pp}}\boldsymbol{\epsilon}^{(k)}_{pG}, \qquad \boldsymbol{\sigma}^{(k)}_{nM} = \bar{\mathrm{C}}^{(k)}_{\mathrm{nn}}\boldsymbol{\epsilon}^{(k)}_{nH}, \tag{16}$$

where

$$\boldsymbol{\epsilon}^{(k)}_{nH} = (\bar{\mathrm{C}}^{(k)}_{\mathrm{nn}})^{-1}\boldsymbol{\sigma}^{(k)}_{nM}, \tag{17}$$

Now we can write the variational formulation for the k-th lamina in the reference problem system as:

$$\begin{aligned} \int_{V_k} \Big[& \delta\boldsymbol{\epsilon}^{(k)}_{pG}\,\bar{\mathrm{C}}^{(k)}_{\mathrm{pp}}\,\boldsymbol{\epsilon}^{(k)}_{pG} + \delta\boldsymbol{\epsilon}^{(k)}_{nG}\boldsymbol{\sigma}^{(k)}_{nM} + \\ & \delta\boldsymbol{\sigma}^{(k)}_{nM}\left(\boldsymbol{\epsilon}^{(k)}_{nG} - (\bar{\mathrm{C}}^{(k)}_{\mathrm{nn}})^{-1}\boldsymbol{\sigma}^{(k)}_{nM}\right)\Big]\, dxdydz = \delta L_e \end{aligned} \tag{18}$$

4. A model for multilayered plates based on FSDT (First-order Shear Deformation Theory) in RMVT

The RMVT approach is suitable to develop two-dimensional modelling of multilayered structures. The behavior of displacements and transverse stresses is expressed in the thickness plate z-direction according to a z power expansion. In this work we use the first order expansion of the Reissner-Mindlin model for the displacements field, while we assume that the transverse stresses are parabolic functions independent in each layer. Thus, referring to the usual notations, we denote our model by the code EM1-2. The previous assumptions correspond to adopt an equivalent single layer description (**ESL**) for the displacements and a layer-wise (**LW**) description for the transverse stresses. In fact, the treatment at the layer level permits an accurate description of the transverse stresses distribution along the thickness of the multilayered plate.

In particular, let $\mathbf{u}$ be the displacements field, $\mathbf{u} = [u_x,\ u_y,\ u_z]$, the Reissner-Mindlin kinematic assumptions are:

$$\begin{aligned} u_x(x,y,z) &= z\,\theta_x(x,y) \\ u_y(x,y,z) &= z\,\theta_y(x,y) \\ u_z(x,y,z) &= w(x,y). \end{aligned} \tag{19}$$

The functions θ_x and θ_y are the rotations of the normal to the undeformed middle surface Ω in the x-z and y-z planes, respectively. Both the transverse displacement and the rotations depend only on (x,y) and thus their description is made at the multilayered level. Note that the membrane displacements are discarded in the expansion of u_x and u_y, although the membrane-bending coupling should be taken into account in anisotropic materials. At a first attempt, the authors want to demonstrate that the present mixed model provides accurate results in terms of transverse shear stresses independently of the displacement field.

The displacement assumptions above lead to express the in-plane and out-plane strains in terms of the rotations and the transverse displacement in this way:

$$\begin{aligned} \boldsymbol{\epsilon}_{pG}(\boldsymbol{\theta}) &= \left[z\frac{\partial\theta_x}{\partial x}, \quad z\frac{\partial\theta_y}{\partial y}, \quad z(\frac{\partial\theta_x}{\partial y} + \frac{\partial\theta_y}{\partial x})\right]^T \\ \boldsymbol{\epsilon}_{nG}(\boldsymbol{\theta}, w) &= \left[\theta_x + \frac{\partial w}{\partial x}, \quad \theta_y + \frac{\partial w}{\partial y}\right]^T, \quad \boldsymbol{\theta} = [\theta_x,\ \theta_y]^T \end{aligned} \tag{20}$$

In order to model the stresses $\boldsymbol{\sigma}^{(k)}_{nM} = [\sigma^{(k)}_{xz},\ \sigma^{(k)}_{yz}]$ in the layer-wise approach we assume that in any k-layer, $k = 1, ...N_l$, the stresses are written in the following form:

$$\begin{aligned} \sigma^{(k)}_{xz} &= F_t(z)\sigma^{(k)}_{xz_t} + F_b(z)\sigma^{(k)}_{xz_b} + F_2(z)\sigma^{(k)}_{xz_2} \\ \sigma^{(k)}_{yz} &= F_t(z)\sigma^{(k)}_{yz_t} + F_b(z)\sigma^{(k)}_{yz_b} + F_2(z)\sigma^{(k)}_{yz_2} \end{aligned} \tag{21}$$

The subscripts t and b denote values related to the k-layer top and bottom surfaces respectively and the thickness

functions $F_t(z),\ F_b(z),\ F_2(z)$ are defined as follows:

$$\begin{aligned} &F_t(z) = \frac{P_0 + P_1}{2}, \quad F_b(z) = \frac{P_0 - P_1}{2}, \\ &F_2(z) = P_2 - P_0, \end{aligned} \tag{22}$$

where $P_j = P_j(z)$ is the Legendre polynomial of $j-$order. By introducing the non-dimensioned layer coordinate τ_k with $-1 \leq \tau_k \leq 1$ the Legendre polynomials are:

$$P_0 = 1, \quad P_1 = \tau_k, \quad P_2 = \frac{3\tau_k^2 - 1}{2} \tag{23}$$

Such a choice makes the model particularly suitable to impose the interlaminar transverse stress continuty (IC) by linking:

$$\begin{aligned} \sigma_{xz_t}^{(k)} &= \sigma_{xz_b}^{(k+1)} \\ \sigma_{yz_t}^{(k)} &= \sigma_{yz_b}^{(k+1)} \end{aligned} \tag{24}$$

for $k = 1, ...N_l - 1$. Moreover, the homogeneous top and bottom conditions are easily imposed.

Finally, by combining the FSDT assumptions with the layer-wise approach (21), the problem (18) will be expressed in each $k-$layer in terms of the $k-$independent variables $\theta_x,\ \theta_y,\ w$ and the variables $\sigma_{xz_t}^{(k)},\ \sigma_{xz_b}^{(k)},\ \sigma_{xz_2}^{(k)},\ \sigma_{yz_t}^{(k)},\ \sigma_{yz_b}^{(k)},\ \sigma_{yz_2}^{(k)}$.
In particular we introduce the suitable spaces: $\boldsymbol{\Theta}$, W and $\boldsymbol{\Sigma}$ of admissible rotations, vertical displacement and transverse stresses respectively.
Let us consider the three-component vector of curvatures $\boldsymbol{\kappa}(\boldsymbol{\theta})$:

$$\boldsymbol{\kappa}(\boldsymbol{\theta}) = \left[\frac{\partial \theta_x}{\partial x}, \quad \frac{\partial \theta_y}{\partial y}, \quad \frac{\partial \theta_x}{\partial y} + \frac{\partial \theta_y}{\partial x}\right]^T \tag{25}$$

and the normal stress vector $\boldsymbol{\sigma}_n^{(k)} = \int_{I_k} \boldsymbol{\sigma}_{nM}^{(k)} dz,\ I_k = [-t_k/2,\ t_k/2]$, namely:

$$\boldsymbol{\sigma}_n^{(k)} = \begin{bmatrix} \sigma_{xz_t}^{(k)} \int_{I_k} F_t(z)dz + \sigma_{xz_b}^{(k)} \int_{I_k} F_b(z)dz + \sigma_{xz_2}^{(k)} \int_{I_k} F_2(z)dz \\ \sigma_{yz_t}^{(k)} \int_{I_k} F_t(z)dz + \sigma_{yz_b}^{(k)} \int_{I_k} F_b(z)dz + \sigma_{yz_2}^{(k)} \int_{I_k} F_2(z)dz \end{bmatrix}. \tag{26}$$

We observe that the normal stress vector can therefore be expressed in terms of the unknowns vectors, $\boldsymbol{\sigma}^t, \boldsymbol{\sigma}^b, \boldsymbol{\sigma}^2$:

$$\begin{aligned} \boldsymbol{\sigma}^t &= [\sigma_{xz_t}^{(k)},\ \sigma_{yz_t}^{(k)}]^T, \\ \boldsymbol{\sigma}^b &= [\sigma_{xz_b}^{(k)},\ \sigma_{yz_b}^{(k)}]^T, \\ \boldsymbol{\sigma}^2 &= [\sigma_{xz_2}^{(k)},\ \sigma_{yz_2}^{(k)}]^T, \\ \boldsymbol{\sigma}_n^{(k)} &= \boldsymbol{\sigma}_n^{(k)}(\boldsymbol{\sigma}^t, \boldsymbol{\sigma}^b, \boldsymbol{\sigma}^2). \end{aligned} \tag{27}$$

Integrating (18) along the thickness of each layer, we obtain the variational formulation of the RMVT model involving FSDT approach:

$$\begin{cases} \text{Find } (\boldsymbol{\theta}, w, \boldsymbol{\sigma}^t, \boldsymbol{\sigma}^b, \boldsymbol{\sigma}^2) \in \boldsymbol{\Theta} \times W \times \boldsymbol{\Sigma}^3 : \\ \dfrac{t_k^3}{12} \displaystyle\int_\Omega \delta\boldsymbol{\kappa}(\boldsymbol{\theta}) \bar{\mathrm{C}}_{\mathrm{pp}}^{(k)} \boldsymbol{\kappa}(\boldsymbol{\theta})\ dx\, dy + \\ \displaystyle\int_\Omega \delta\boldsymbol{\epsilon}_{nG}(\boldsymbol{\theta}, w) \boldsymbol{\sigma}_n^{(k)}(\boldsymbol{\sigma}^t, \boldsymbol{\sigma}^b, \boldsymbol{\sigma}^2) dx\, dy = \delta L_e \\ \displaystyle\int_\Omega \delta\boldsymbol{\sigma}_n^{(k)}(\boldsymbol{\sigma}^t, \boldsymbol{\sigma}^b, \boldsymbol{\sigma}^2) \boldsymbol{\epsilon}_{nG}(\boldsymbol{\theta}, w)\ dx\, dy - \\ \displaystyle\int_\Omega \delta\boldsymbol{\sigma}_n^{(k)}(\boldsymbol{\sigma}^t, \boldsymbol{\sigma}^b, \boldsymbol{\sigma}^2) (\bar{\mathrm{C}}_{\mathrm{nn}}^{(k)})^{-1} \boldsymbol{\sigma}_n^{(k)}(\boldsymbol{\sigma}^t, \boldsymbol{\sigma}^b, \boldsymbol{\sigma}^2) dx\, dy = 0 \end{cases} \tag{28}$$

Finally, in order to fully describe the multilayered structure it is necessary to assemble the N_l problems (28), holding in each layer.

5. Finite element approximation

In this paper we introduce an advanced locking-free finite element to treat the multilayered plates. We consider a strategy similar to MITC approach tailored to the RMVT formulation.
Let we introduce a shape regular and conforming rectangular grid $\mathcal{T}_h$ of elements of diameter h for the domain Ω, which we assume rectangle for simplicity. The reliability of these elements in terms of mesh distortion, already demonstrated in [43] for mixed elements based on displacement formulation, will be evaluated in future companion works. We consider a particular MITC finite element, known as MITC9 (see [44]). This element is characterized by the following choice of the finite element spaces:

$$\begin{aligned} &\boldsymbol{\Theta}_h \subset \boldsymbol{\Theta}, \qquad \boldsymbol{\Theta}_h = \Theta_h \times \Theta_h, \\ &W_h \subset W, \qquad \boldsymbol{\Sigma}_h \subset \boldsymbol{\Sigma}. \end{aligned} \tag{29}$$

More precisely we set:

$$\Theta_h = \left\{ v \in H^1(\Omega)\ :\ v|_{\mathcal{Q}} \in Q_2(\ \mathcal{Q}) \ \forall\ \mathcal{Q} \in \mathcal{T}_h \right\} \tag{30}$$

where $Q_2(\ \mathcal{Q})$ is the space of polynomials of degree at most 2 in each variable,

$$W_h = \left\{ v \in H^1(\Omega)\ :\ v|_{\ \mathcal{Q}} \in S_2(\ \mathcal{Q}) \ \forall\ \mathcal{Q} \in \mathcal{T}_h \right\} \tag{31}$$

where $S_2(\ \mathcal{Q})$ denotes the space of serendipity polynomials of degree 2,

$$\begin{aligned} \boldsymbol{\Sigma}_h = \big\{ &\mathbf{s}\ :\ \mathbf{s}_{|\ \mathcal{Q}} \in \Sigma_x \times \Sigma_y \ \forall\ \mathcal{Q} \in \mathcal{T}_h, \\ &\mathbf{s} \cdot \boldsymbol{\tau} \ \text{ continuous at the interelement boundaries} \big\} \end{aligned} \tag{32}$$

where $\boldsymbol{\tau}$ is the tangential unit vector to each edge of each element $\mathcal{Q}$,

$$\Sigma_x = Q_1(\ \mathcal{Q}) + \mathrm{span}\{y^2\}$$

and

$$\Sigma_y = Q_1(\ \mathcal{Q}) + \mathrm{span}\{x^2\}.$$

The degrees of freedom for the spaces Θ_h and W_h on each element are the usual ones. The shape functions for the local spaces Σ_x and Σ_y are uniquely determined by suitable degrees of freedom as described in ([36],[39]). The Figure 2 shows the degrees of freedom for the approximate spaces.

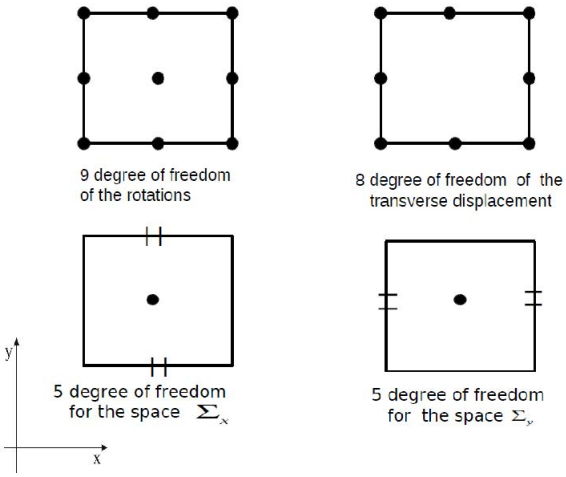

Figure 2: Degrees of freedom for the approximate spaces

Under these choices the problem (28) is discretized layer by layer in the following way:

$$\begin{cases} \text{Find } (\boldsymbol{\theta}_h, w_h, \boldsymbol{\sigma}_h^t, \boldsymbol{\sigma}_h^b, \boldsymbol{\sigma}_h^2) \in \boldsymbol{\Theta}_h \times W_h \times (\boldsymbol{\Sigma}_h)^3 : \\ \dfrac{t_k^3}{12} \displaystyle\int_\Omega \delta\boldsymbol{\kappa}(\boldsymbol{\theta}_h) \bar{\mathrm{C}}_{\mathrm{pp}}^{(k)} \boldsymbol{\kappa}(\boldsymbol{\theta}_h)\, dx\, dy + \\ \displaystyle\int_\Omega \delta\boldsymbol{\epsilon}_{nG}(\boldsymbol{\theta}_h, w_h) \boldsymbol{\sigma}_n^{(k)}(\boldsymbol{\sigma}_h^t, \boldsymbol{\sigma}_h^b, \boldsymbol{\sigma}_h^2) dx\, dy = \delta L_e \\ \displaystyle\int_\Omega \delta\boldsymbol{\sigma}_n^{(k)}(\boldsymbol{\sigma}_h^t, \boldsymbol{\sigma}_h^b, \boldsymbol{\sigma}_h^2) \boldsymbol{\epsilon}_{nG}(\boldsymbol{\theta}_h, w_h)\, dx\, dy - \\ \displaystyle\int_\Omega \delta\boldsymbol{\sigma}_n^{(k)}(\boldsymbol{\sigma}_h^t, \boldsymbol{\sigma}_h^b, \boldsymbol{\sigma}_h^2) (\bar{\mathrm{C}}_{\mathrm{nn}}^{(k)})^{-1} \boldsymbol{\sigma}_n^{(k)}(\boldsymbol{\sigma}_h^t, \boldsymbol{\sigma}_h^b, \boldsymbol{\sigma}_h^2) dx\, dy = 0 \end{cases} \tag{33}$$

In Figure 3 we show the structure of the stiffness matrix related to the problem (33). In particular, we point out the differences between the anisotropic and the isotropic case. The assembling of the stiffness matrix at multilayer-level is carried out by summing the stiffness matrices of the layers where the **ESL** description is used (rotations and transverse displacement) and by imposing the continuity conditions when the shear stresses are taken into account. Finally in the approximation of the multilayered plate problem with our model EM1-2, the vertical displacement and the rotations are constant along the thickness, while the transverse shear stresses are parabolic on each layer and they are linked together by the interlaminar stress continuity condition. Due to the polynomial spaces chosen for the FEM approximation, the continuity between adjacent elements is not directly imposed for the transverse shear stresses.

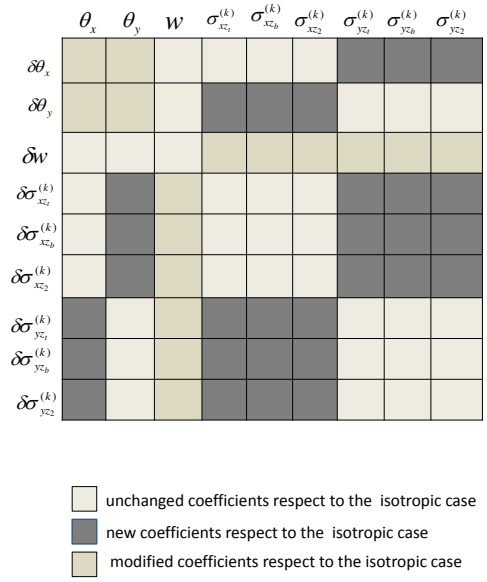

Figure 3: Stiffness matrix for k-layer

6. Numerical results

In order to assess the implemented finite element EM1-2 a large numerical investigation is conducted. We present the convergence studies and the comparison to three-dimensional exact analysis and to other available finite element results. Different types of multilayered plates are treated, in particular a symmetric cross-ply plate ($90^{\mathrm{O}}/0^{\mathrm{O}}/90^{\mathrm{O}}$) and two antisymmetric angle-ply laminates ($-45^{\mathrm{O}}/45^{\mathrm{O}}$) and ($0^{\mathrm{O}}/60^{\mathrm{O}}$). The mechanical properties of the used laminae are the following:

$$\begin{aligned} &E_1 = 25\,GPa,\ E_2 = 1\,GPa, \\ &G_{12} = G_{13} = 0.5\,GPa,\ G_{23} = 0.2\,GPa \\ &\nu_{12} = 0.25, \end{aligned} \tag{34}$$

let a and b be the dimensions of the lamina of thickness t as indicated in Figure 4. The vertical displacement and the stresses are normalized according to the formula:

$$\begin{aligned} &\bar{w} = w \frac{100 E_2 t^3}{p_z a^4} \\ &\bar{\sigma}_{xz} = \frac{\sigma_{xz}}{p_z(a/t)}, \quad \bar{\sigma}_{yz} = \frac{\sigma_{yz}}{p_z(a/t)}. \end{aligned} \tag{35}$$

Different loadings as well as boundary conditions are considered and an analysis of locking phenomenon is presented. The achieved results show a good numerical performance of our EM1-2 model.

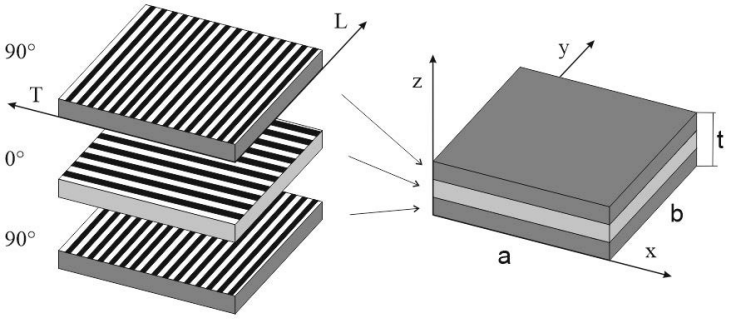

Figure 4: Multilayered structure geometry

Table 1: Vertical displacement of $(90^{\mathrm{O}}/0^{\mathrm{O}}/90^{\mathrm{O}})$ laminate

a/t	3D	EM1-2	FSDT
4	2.820	2.2204	2.0547
10	0.919	0.77996	0.75315
20	0.610	0.5726	0.5659
100	0.508	0.5061	0.5059
1000		0.5034	0.5034

6.1. Cross-ply symmetrical plate $(90^{\mathrm{O}}/0^{\mathrm{O}}/90^{\mathrm{O}})$

We consider a simply-supported laminate loaded with a bisinusoidal uniformly distributed pressure applied at the top surface:

$$\mathbf{p} = (0, 0, p_z), \quad p_z(x, y) = \sin\left(\frac{\pi x}{a}\right) \sin\left(\frac{\pi y}{b}\right). \tag{36}$$

The geometrical properties are:

$$a = 1\,m,\ b = 3\,m,\ t_k = \frac{1}{3}t,\ k = 1, 2, 3, \tag{37}$$

In Table 1 we report the vertical displacement $\bar{w}$ evaluated at the point $(a/2, b/2, 0)$ for $a/t = 4 \div 1000$ by our EM1-2 model compared with the 3D solution (see [45]) and classical FSDT theory (with 'classical' we mean that the membrane displacements are included). A uniform mesh 5×5 is considered. In Figures 5 and 6 the behaviour of the transverse shear stress $\bar{\sigma}_{xz}$ at the points $(0, b/2, z/t)$ is shown for $a/t = 4$ and $a/t = 1000$ respectively. We compare the results with those obtained with Layer-wise Mixed model of fourth order (LM4) that can be used as a quasi-3D solution. We present also the comparison with the FSDT model to validate the improvement of the solution obtained by our EM1-2 model. Analogously, in Figures 7 and 8 the behaviour of the transverse shear stress $\bar{\sigma}_{yz}$ at the points $(a/2, 0, z/t)$ is shown for $a/t = 4$ and $a/t = 1000$ respectively. In Figure 9 we show that the EM1-2 approach leads to a locking-free finite element to treat the orthotropic multilayered plate.

6.2. Antisymmetric angle-ply plate $(-45^{\mathrm{O}}/45^{\mathrm{O}})$

We consider two simply-supported square plates ($a = b = 1$) with lay-out $(-45^{\mathrm{O}}/45^{\mathrm{O}})$ and thicknesses $t_k = \frac{1}{2}t,\ k = 1, 2$. One plate is subjected to a uniformly distributed (UD) load and the other is subjected to the sinusoidally distributed (SSL) load (36). We analyze the effect of the lamination scheme and the shear deformation on the transverse stresses. In Table (2) a convergence study with different mesh sizes is presented in terms of transverse shear stresses $\bar{\sigma}_{xz}$ at the point $(0, b/2, 1/4)$, in both the cases of load UD and SSL and thickness ratios $a/t = 4, 1000$. It is demonstrated that the results converge for the mesh 12×12 and this last is used for the following analyses. Then, in Table 3 we compare our numerical results with those obtained in [46] for the thickness ratios $a/t = 10, 20, 100, 1000$. Moreover, we show the behaviour of the transverse shear stresses $\bar{\sigma}_{xz}$ and $\bar{\sigma}_{yz}$ at the points $(0, b/2, z/t)$ and $(a/2, 0, z/t)$ respectively, in the case of bisinusoidally distributed load. We consider both the cases $a/t = 10$ and $a/t = 1000$. In Figures 10 and 11 the stresses $\bar{\sigma}_{xz}$ obtained by EM1-2 model and FSDT approach are shown and in Figures 12 and 13 the stresses $\bar{\sigma}_{yz}$ are represented. We remark that the results obtained by EM1-2 model are in agreement with the results reported

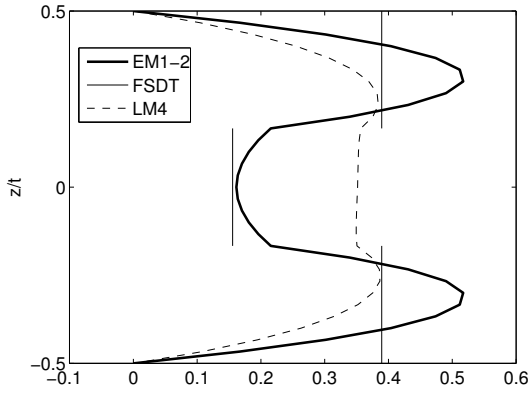

Figure 5: Shear stress $\bar{\sigma}_{xz}$ of $(90^{\mathrm{O}}/0^{\mathrm{O}}/90^{\mathrm{O}})$ laminate for $a/t = 4$

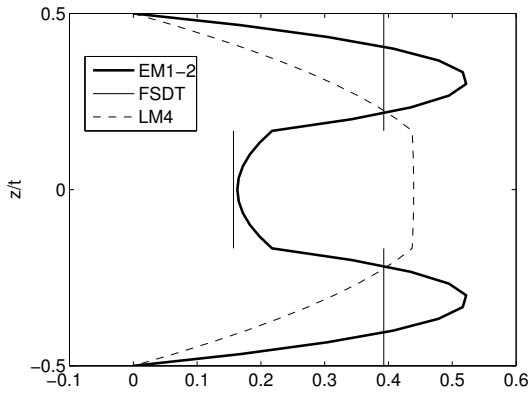

Figure 6: Shear stress $\bar{\sigma}_{xz}$ of $(90^{\mathrm{O}}/0^{\mathrm{O}}/90^{\mathrm{O}})$ laminate for $a/t = 1000$

Table 2: Transverse shear stresses $\bar{\sigma}_{xz}$, $(-45^{\mathrm{O}}/45^{\mathrm{O}})$ laminate

a/t		EM1-2				
	n	4×4	6×6	8×8	12×12	14×14
4	UD	0.4249	0.4371	0.4432	0.4472	0.4480
	SSL	0.2068	0.2110	0.2124	0.2133	0.2135
1000	UD	0.4189	0.4188	0.4275	0.4293	0.4297
	SSL	0.2098	0.2112	0.2131	0.2137	0.2138

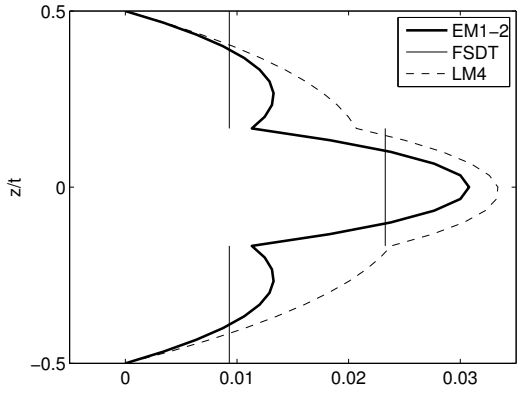

Figure 7: Shear stress $\bar{\sigma}_{yz}$ of cross-ply symmetrical plate $(90^{\mathrm{O}}/0^{\mathrm{O}}/90^{\mathrm{O}})$ for $a/t = 4$

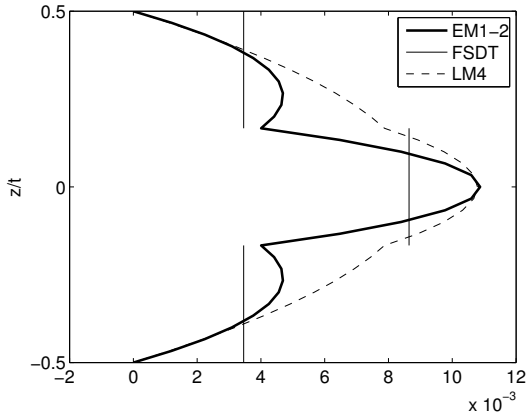

Figure 8: Shear stress $\bar{\sigma}_{yz}$ of $(90^{\mathrm{O}}/0^{\mathrm{O}}/90^{\mathrm{O}})$ laminate for $a/t = 1000$

Table 3: Transverse shear stresses $\bar{\sigma}_{xz}$, $(-45^{\mathrm{O}}/45^{\mathrm{O}})$ laminate

a/t	load	Reddy	EM1-2
10	UD	0.4238	0.4382
	SSL	0.2143	0.2134
20	UD	0.4205	0.4318
	SSL	0.2143	0.2134
100	UD	0.4189	0.4286
	SSL	0.2143	0.2135
1000	UD		0.4293
	SSL		0.2137

by Reddy in Figures 6.4.4 and 6.4.5 of [46]. We observe that unlike in antisymmetric cross-ply laminates the stress $\bar{\sigma}_{yz}$ is not zero at $(0, b/2, z/t)$ although small compared to that at $(a/2, 0, z/t)$.

The robustness of our element respect to the locking phenomenon is shown in Figure 14, where the transverse displacement is plotted for very thin laminates. Although the comparison with classical FSDT solution highlights a drawback of the present model in the description of the displacements, it is demonstrated that EM1-2 element is locking free in the analysis of anisotropic plates.

6.3. Antisymmetric angle-ply plate $(0^{\mathrm{O}}/60^{\mathrm{O}})$

We consider a square plate $(a = b = 1)$ with lay-out $(0^{\mathrm{O}}/60^{\mathrm{O}})$ and thicknesses $t_k = \frac{1}{2}t,\ k = 1, 2$, subjected to a uniformly distributed load. We analyze such a laminated plate with arbitrary combination of boundary conditions and we compare our results with those presented in [47]. We denote by F,C and S the free, clamped and simply supported boundary conditions respectively. More

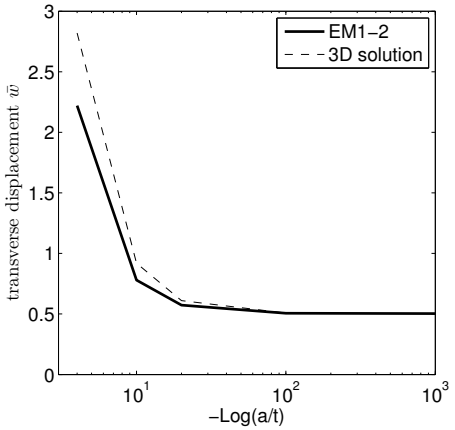

Figure 9: Transverse displacement $\bar{w}$ of $(90^{\mathrm{O}}/0^{\mathrm{O}}/90^{\mathrm{O}})$ laminate versus the thickness

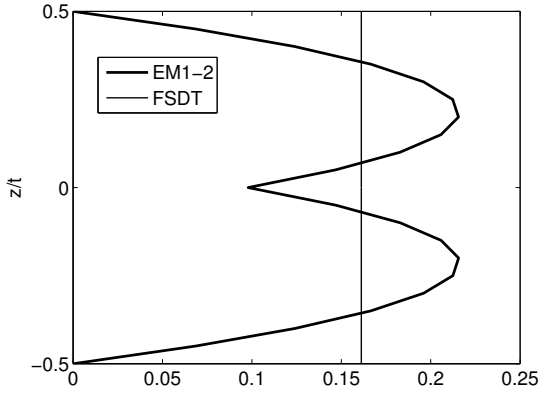

Figure 10: Shear stress $\bar{\sigma}_{xz}$ of $(-45^{\mathrm{O}}/45^{\mathrm{O}})$ laminate for $a/t = 10$

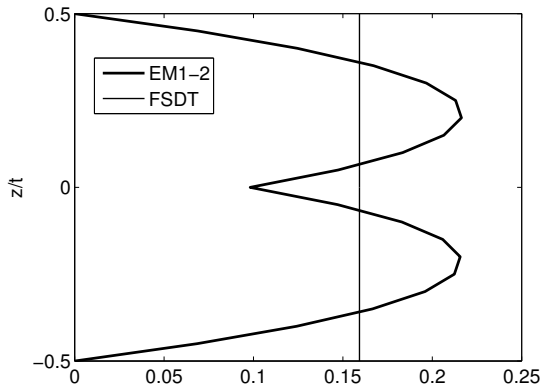

Figure 11: Shear stress $\bar{\sigma}_{xz}$ of $(-45^{\mathrm{O}}/45^{\mathrm{O}})$ laminate for $a/t = 1000$

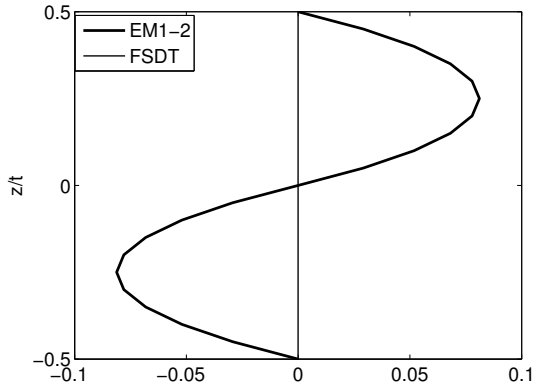

Figure 12: Shear stress $\bar{\sigma}_{yz}$ of $(-45^{\mathrm{O}}/45^{\mathrm{O}})$ laminate for $a/t = 10$

specifically for antisymmetric angle-ply laminates the simply supported conditions are:

$$\begin{aligned} w = \theta_x = 0 \quad &\text{at } x = 0,\ x = a \\ w = \theta_y = 0 \quad &\text{at } y = 0,\ y = b \end{aligned} \tag{38}$$

We use a 4-word notation, such as CCSF, to indicate the boundary conditions on the four edges of the plates ordered in this way: $x = 0$, $y = 0$, $x = a$, $y = b$. In Figure 15 we report the transverse shear stresses $\bar{\sigma}_{yz}$ at $(a/4, b/4, z/t)$ obtained by our EM1-2 model related to $a/t = 10$ and three different boundary conditions: CFCC, SCCS, SCFF. The results are in agreement with those reported by Naserian Nik and Tahani in Figure 7(a) of [47]. In Figure 16 we report the transverse shear stresses $\bar{\sigma}_{xz}$ at $(a/4, b/4, z/t)$ obtained by our model related to $a/t = 10$ and three different boundary conditions: CFFC, CSCS, FCSS. Also these results are in agreement with those reported in Figure 7(b) of [47]. In order to test the robustness of EM1-2 element with respect to the locking phenomenon we analyze the behaviour of the transverse displacement, the transverse shear stresses $\bar{\sigma}_{yz}$ and $\bar{\sigma}_{xz}$ at $(a/4, b/4, z/t)$ when $a/t = 10, 100, 1000$ for meaningful cases of boundary conditions. In particular, in Figures 17, 18 and 19 a locking study for transverse displacement w and transverse stresses $\bar{\sigma}_{yz}$, $\bar{\sigma}_{xz}$ in the SCCS case is presented. Also here, the discrepancy with classical FSDT solution is present but EM1-2 element doesn't show locking in the analysis of very thin anisotropic plates (see Fig. 17).

7. Conclusions

This work presents the analysis of anisotropic multilayered plates by means of an advanced locking-free finite element (EM1-2). The problem is modelled by adopting the variational formulation based on RMVT. A mixed theory with equivalent single layer (ESL) descriptions for the displacements and a layerwise (LW) description for the transverse stresses is considered. In particular a first order displacements field in conjunction with a parabolic transverse stresses field independent in each layer is adopted. The continuity condition of the transverse shear stresses at

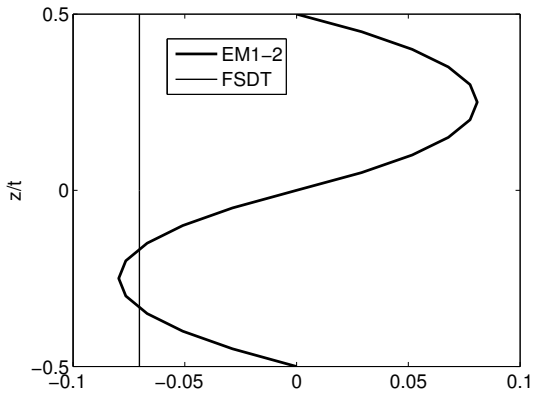

Figure 13: Shear stress $\bar{\sigma}_{yz}$ of $(-45^{\mathrm{O}}/45^{\mathrm{O}})$ laminate for $a/t = 1000$

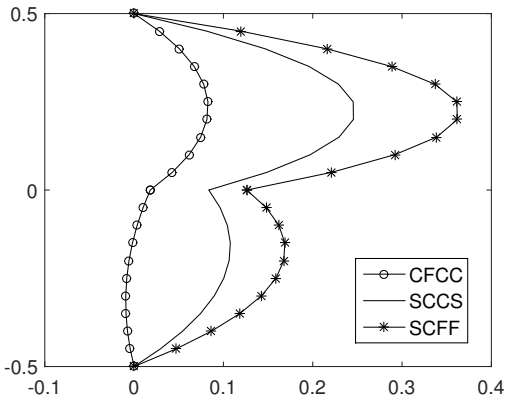

Figure 15: Shear stress $\bar{\sigma}_{yz}$ of $(0^{\mathrm{O}}/60^{\mathrm{O}})$ laminate for $a/t = 10$

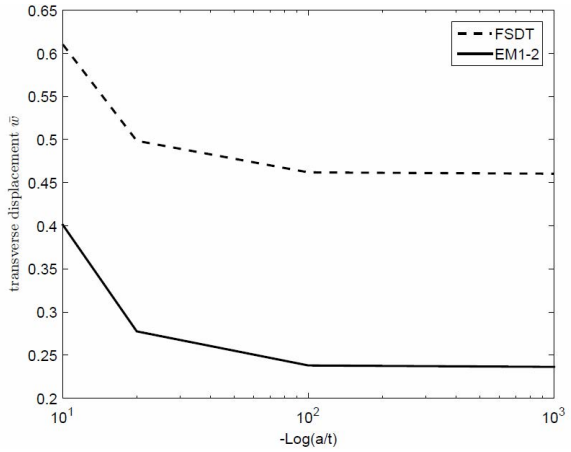

Figure 14: Transverse displacement $\bar{w}$ of $(-45^{\mathrm{O}}/45^{\mathrm{O}})$ laminate versus the thickness

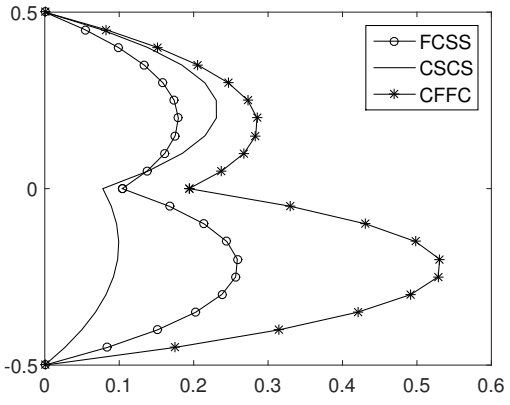

Figure 16: Shear stress $\bar{\sigma}_{xz}$ of $(0^{\mathrm{O}}/60^{\mathrm{O}})$ laminate for $a/t = 10$

the interfaces between layers (IC) is easily imposed by assuming the stresses as independent variables. The in-plane approximation is performed by a strategy similar to MITC (Mixed Interpolated Tensorial Components) finite element approach in order to contrast the locking. Due to the polynomial spaces chosen for the FEM approximations, the continuity of transverse shear stresses is not imposed between adjacent elements. Different benchmark tests of multilayered composite plates are considered to validate both properties of convergence and robustness of the element EM1-2 with respect to the 3D solutions, even in the case of anisotropic structures. Although the comparison with the FSDT solution highlights a drawback of the present model in the description of the displacements that will be overcome in future companion works, EM1-2 results show an improvement in terms of transverse shear stresses with respect to the piecewise constant FSDT approximations. The analysis of the solution performed versus the thickness of the structure for different boundary conditions and different thickness ratios confirms that EM1-2 is a locking-free finite element able to provide convergent and accurate results even for multilayered plates with very high degree of anisotropy.

References

[1] Lekhnitskii S.G. Anisotropic Plates. Gordon and Breach, New York, Translated from the second Russian edition by S. W. Tsai and T. Cheron 1968;273-491.

[2] Hearmon R.F.S. An Introduction to Applied Anisotropic Elasticity. Oxford University Press, New York 1969;90-127.

[3] Ashton J.E., Whitney J.M. Theory of laminated plates. Technomic, Stamford, Conn. 1970.

[4] Stavsky Y. Bending and Stretching of Laminated Aelotropic Plates. J of Eng Mech Divis, ASCE 1961;87(6):31-56.

[5] Dong S.B., Pister K.S., Taylor R.L. On the Theory of Laminated Anisotropie Shells and Plates. J of Aeros Scien 1962; 969-974.

[6] Whitney J.M. The effects of transverse shear deformation on the bending of laminated plates. J Compos Mat 1969;3:534-547.

[7] Pagano N. J. Exact solutions for Composite Laminates in Cylindrical Bending. J Compos Mat 1969;3:398-411.

[8] Reissner E. On a certain mixed variational theory and a proposed application. Int J Numer Methods Eng 1984;20:13661368.

[9] Reissner E. On a mixed variational theorem and on a shear deformable plate theory. Int J Numer Methods Eng 1986;23:193198.

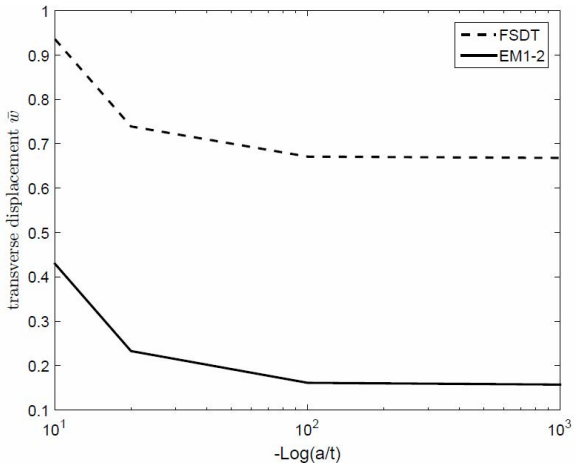

Figure 17: Transverse displacement $\bar{w}$ of $(0^{\mathrm{O}}/60^{\mathrm{O}})$ laminate versus the thickness SCCS b.c.

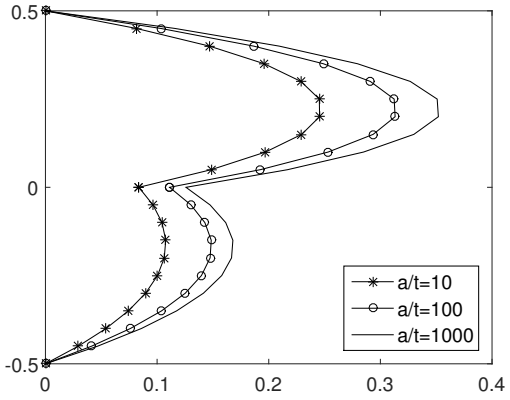

Figure 18: Transverse shear stress $\bar{\sigma}_{yz}$ of $(0^{\mathrm{O}}/60^{\mathrm{O}})$ laminate versus the thickness SCCS b.c.

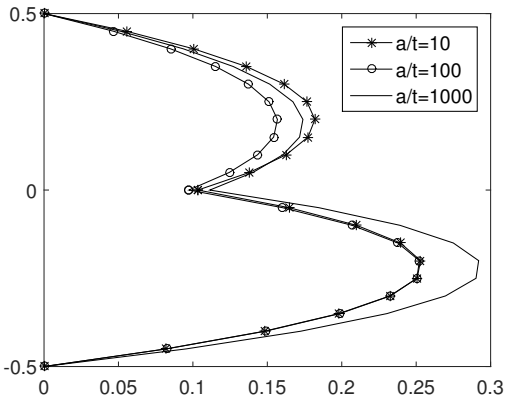

Figure 19: Transverse shear stress $\bar{\sigma}_{xz}$ of $(0^{\mathrm{O}}/60^{\mathrm{O}})$ laminate versus the thickness SCCS b.c.

[10] Reissner E. On a certain mixed variational theorem and on a laminated elastic shell theory. Proc of Euromech-Colloquium 1986;219:1727.

[11] Carrera E. Developments, ideas, and evaluations based upon Reissners Mixed Variational Theorem in the modeling of multilayered plates and shells. Appl Mech Rev 2001;54(4):301329.

[12] Murakami H. Laminated composite plate theory with improved in-plane responses. ASME Proc of PVP Conf, New Orleans 1985;98-2:257263.

[13] Murakami H. Laminated composite plate theory with improved in-plane responses. ASME J Appl Mech 1986;53:661666.

[14] Toledano A., Murakami H. A high-order laminated plate theory with improved in-plane responses. Int J Solids Struct 1987;23:111131.

[15] Toledano A., Murakami H. A composite plate theory for arbitrary laminate configurations. ASME J Appl Mech 1987;54:181189.

[16] Soldatos K.P. Cylindrical bending of cross-ply laminated plates: refined 2D plate theories in comparison with the exact 3D elasticity solution. Tech Report 140, Dept. of Math., University of Ioannina, Greece.

[17] Carrera E. A class of two-dimensional theories for anisotropic multilayered plates analysis. Accademia delle Scienze di Torino, Memorie Scienze Fisiche 1995;19-20:139.

[18] Carrera E. C_0^z Requirements-models for the two dimensional analysis of multilayered structures. Compos Struct 1997;37:373384.

[19] Carrera E. Recent Developments in the Modeling of Multilayered Plates and Shells based upon Reissner's Mixed Equation. In: XIV congresso AIMETA, Como 6-9 October 1999.

[20] Carrera E. A Reissner's mixed variational theorem applied to vibration analysis of multilayered shells. ASME J Appl Mech Como 1999;66:6978.

[21] Carrera E. Mixed layer-wise models for multilayered plates analysis. Compos Struct 1998;43:5770.

[22] Carrera E. Evaluation of layer-wise mixed theories for laminated plates analysis. AIAA J 1998;26:830839.

[23] Carrera E. Transverse normal stress effects in multilayered plates. ASME J Appl Mech 1999;66:10041012.

[24] Carrera E. A study of transverse normal stress effects on vibration of multilayered plates and shells. J Sound Vib 1999;225:803-829.

[25] Carrera E. Single-layer vs multi-layers plate modelings on the basis of Reissners mixed theorem. AIAA J 2000;38(2):342352.

[26] Carrera E. A priori vs a posteriori evaluation of transverse stresses in multilayered orthotropic plates. Compos Struct 2000;48:245-260.

[27] Carrera E. Vibrations of layered plates and shells via Reissner's Mixed Variational Theorem. In: Fourth Symposiom on Vibrations of Continuos Systems, Kenswick, 2003, July 7-11, 4-6.

[28] Carrera E. Layer-wise mixed models for accurate vibration analysis of multilayered plates. ASME J Appl Mech 1998;65:820828.

[29] Messina A. Two generalized higher order theories in free vibration studies of multilayered plates. J Sound Vib 2001;242:125150.

[30] Carrera E., Demasi L. Sandwich plates analyses by finite element method and Reissner's Mixed Theorem. In: Sandwich V, Zurich, 2000, September 5-7, 301-313.

[31] Carrera E., Demasi L. Multilayered finite plate element based on Reissner Mixed Variational Theorem. Part I: Theory. Int J Numer Meth Eng 2002;55:191-231.

[32] Carrera E., Demasi L. Multilayered finite plate element based on Reissner Mixed Variational Theorem. Part II: Numerical Analysis. Int J Numer Meth Eng 2002;55:253-296.

[33] Zienkiewicz O.C., Taylor R.L., Too J.M. Reduced integration techniques in general analysis of plates and shells. Int J Numer Meth Eng 1971;3:275-290.

[34] Huang H.-C. Membrane locking and assumed strain shell elements. Comput Struct 1987;27(5):671-677.

[35] Brezzi F., Bathe K.-J., Fortin M. Mixed-interpolated elements for Reissner-Mindlin plates. Int J Numer Meth Eng 1989;28:1787-1801.

[36] Chinosi C., Della Croce L. Mixed-interpolated elements for thin shell. Commun Numer Meth Eng 1998;14:1155-1170.

[37] Bathe K.-J., Lee P.-S., Hiller J.-F. Towards improving the MITC9 shell element. Comput Struct 2003;81:477-489.

[38] Panasz P., Wisniewski K. Nine-node shell elements with 6 dofs/node based on two-level approximations. Part I Theory and linear tests. Fin Elem Anal Design 2008;44:784-796.
[39] Cinefra M., Chinosi C., Della Croce L. MITC9 shell elements based on refined theories for the analysis of isotropic cylindrical structures. Mech Adv Mater Struct, DOI:10.1080/15376494.2011.581417.
[40] Chinosi C., Cinefra M., Della Croce L., Carrera E. Reissners mixed variational theorem toward MITC finite elements for multilayered plates. Compos Struct, 2013;99:443-452.
[41] Reissner E. The effect of transverse shear deformation on the bending of elastic plates. ASME J Appl Mech 1945;12:69-76.
[42] Mindlin R.D. Influence of rotatory inertia and shear in flexural motions of isotropic elastic plates. ASME J Appl Mech 1951;18:1031-1036.
[43] Della Croce L., Scapolla T. Effect of mesh distortion on Serendipity and mixed finite element solution of thin shells. Int. Journal of Applied Sc. & Computations 1999;5(3):220-237.
[44] Bathe K.-J., Brezzi F., Cho W. The MITC7 and MITC9 plate bending elements. Comput Struct 1989;32:797-841.
[45] Demasi L. Three Dimensional Closed Form Solution and Exact Thin Plate Theories for Isotropic Plates. Compos Struct 2007;80:183-195.
[46] Reddy J.N. Mechanics of Laminated Composite Plates and Shells: Theory and Analysis (2nd Ed.), CRC Press LLC, 2003
[47] Naserian Nik A.M., Tahani M., Analytical solutions for bending analysis of rectangular laminated plates with arbitrary lamination and boundary conditions. Journal of Mechanical Science and Technology 2009;23:2253-2267.